Structural and Thermal Characterization of Hybrid Materials Based on TEOS and DCN

M. Trejo-Durán,[1] A. Martínez-Richa,[2] R. Vera-Graziano,[3] E. Alvarado-Méndez,[1] V. M. Castaño[4]

[1]*Facultad de Ingeniería Mecánica, Eléctrica y Electrónica, Universidad de Guanajuato, Carr. Salamanca-Valle de Santiago Km. 3.5+1.8, Comunidad Palo Alto, Salamanca, Gto. México*
[2]*Facultad de Química, Universidad de Guanajuato, Noria Alta s/n, Guanajuato, Gto., 36050 México*
[3]*Instituto de Investigaciones en Materiales, UNAM, Apdo. Postal 70-360, Coyoacán, 04510, México, D.F*
[4]*Centro de Física Aplicada y Tecnología Avanzada, UNAM, Apdo. Postal 1010, Querétaro, Qro. 76001, México*

Received 27 November 2006; accepted 26 July 2008
DOI 10.1002/app.29110
Published online 13 October 2008 in Wiley InterScience (www.interscience.wiley.com).

ABSTRACT: Solution and solid-state Silicon-29 NMR spectroscopy, X-ray diffraction (WAXS), infrared spectroscopy (IR), thermogravimetric analysis (TGA), and differential scanning calorimetric were used for the characterization of organic–inorganic hybrids, obtained from 4-[[5-dichloromethylsilyl]pentyl]oxy]-cyanobenzene (DCN) and tetraethoxysilane (TEOS). Presence of reaction intermediates during chemical reactions was characterized by NMR. The hybrids are mainly composed of a siloxane copolymer with silicate units. Copolymer has pendant groups of pentyl-oxy-cyanobenzene that behave as chromophores. The nature of ordered–disordered phases was analyzed by X-ray diffraction, differential scanning calorimetry, and thermogravimetric analysis. Ordered phase has a mesogenic structure containing the siloxane copolymer. The disordered phase is mainly silica glass. Molecular modeling for an idealized section of the copolymer suggests that pentyl-oxy-cyanobenzene side-chains align as rigid mesogens along the polymer backbone. Hybrids present self diffraction patterns in coherent luminous rings forms. These patterns indicate the presence of nonlinear optic (NLO) properties. J Appl Polym Sci 111: 794–804, 2009

Key words: organic–inorganic hybrids; chromophores; self-diffraction; NLO-properties; polysiloxanes; pentyl-oxy-cyanobenzene

INTRODUCTION

Electronic, solar, and optoelectronic material industries are steadily growing. The Industrial Development Bureau in USA predicts a continuous growth of this market and in some districts such as Taiwan, domestic trade for these materials will increase nearly three times by 2015, reaching 1 trillion NTD (New Taiwan Dollars).[1] For example, organic LEDs are now produced at commercial scale. Other applications of these materials include sensors, materials used for laser technology, filters, modulators, attenuators, and switches. Materials based on modified silsesquioxanes,[2,3] ormosils,[4,5] and those containing liquid crystals, chromophores, and other ordered organic compounds, usually obtained by sol–gel, have been investigated for the above applications.[6–20]

Anisotropic molecules that are able to form liquid crystalline phases (mesophases) are amenable for electronic and electro-optic applications. Mesogens development for ferroelectric liquid crystals (FLC) and polymer dispersed liquid crystals (PDLC) with nonlinear optics (NLO) properties have drawn attention because of their potential applications. Numerous compounds have been synthesized and their mesomorphic properties have been determined. Particularly, the development of new hybrid materials with NLO properties has received much interest lately because their process for manufacturing optoelectronic devices is straightforward.[20]

In this work, the structure and properties of hybrids obtained from 4-[[5-dichloromethylsilyl]pentyl]oxy]-cyanobenzene (DCN) and tetraethoxysilane (TEOS) by sol–gel process are reported. Hybrids were characterized by FTIR, solid-state NMR, differential scanning calorimetric (DSC), WAXD, and optical techniques. Evidence of mesogenic arrangements in the hybrids is discussed. The diffraction patterns obtained show that hybrids present electro-optical properties. Molecular modeling indicates that the geometrical spatial arrangement of a hybrid idealized

Correspondence to: A. Martínez-Richa (richa@quijote.ugto.mx).

Contract grant sponsor: Consejo de Ciencia y Tecnología del Estado de Guanajuato; contract grant numbers: 07-16-K662-061 A07, GTO-000115-06, GTO-04-C02-104.

Contract grant sponsors: Universidad de Guanajuato (UG), Consejo Nacional de Ciencia y Tecnología (CONACYT; contract grant number: S52740-F.

structure is similar to those observed in other siloxane copolymers with groups having NLO-properties.

EXPERIMENTAL

Materials

5-bromo-1-pentene, 4-cyanophenol, anhydrous potassium carbonate, chloroplatinic acid, toluene, tetraethoxysilane (TEOS), and dimethyldichlorosilane were used as received (Aldrich). Solvents were of commercial grade.

Nuclear magnetic resonance

A Varian Unity *Plus* 300 spectrometer was used to obtain the solution ^{29}Si-NMR spectra in Chloroform-*d* ($CDCl_3$) at room temperature. Insensitive nuclei enhanced by polarization transfer (INEPT) was used to obtain ^{29}Si-NMR spectra, with tetramethylsilane, TMS, as an internal reference. Solid-state ^{29}Si-NMR spectra were recorded under proton decoupling on the same spectrometer. Approximately 100 mg of solid was packed into a 7-mm-diameter zirconium rotor with Kel-F packs. CP-MAS spectra were obtained under Hartmann-Hahn matching conditions and a spinning rate of 4.5 kHz was used. A contact time of 1 ms and a repetition time of 4 s were used. The measurements were made using spin-lock power in radiofrequency units of 60 kHz and typically 4000 transients were recorded. For MAS spectra, a repetition time of 20 s was used. ^{29}Si chemical shifts were referenced to the talc peak at -90 ppm (both in respect with TMS), as determined on a separate sample.

X-ray diffraction

X ray diffraction patterns were recorded on a Siemens D-500 WAXS diffractometer using a CuKα_1 source of 1.5406 Å.

Thermal analysis

Analysis by DSC was performed on a Meter Toledo Star DSC 820e calorimeter previously calibrated with indium. DSC analysis of the samples was made as follows: For DCN monomer, the initial temperature was fixed to -40°C for 10 min, temperature was increased at rate of 10°C/min to 200°C. For hybrids and oligomers, the procedure was similar, but the range of temperatures was 0 to 250°C. After reaching 250°C, the sample was cooled at the same rate to 0°C and heated once more to 250°C. The glass transition temperature was calculated at the heat capacity change midpoint.

Infrared spectroscopy

FTIR spectra were obtained using KBr pellets and films deposited over KBr on a Perkin–Elmer 1600 series spectrometers. Typically, 16 scans were used to record spectra.

Nonlinear optical properties

A continuous argon laser source ($\lambda = 514$ nm) of variable power mounted on an optical bench and a lens of 10 cm of focal distance were used to analyze the nonlinear refractive index.

Minimum energy structure

To determine the minimized energy structure of an idealized section of the copolymer, Alchemy 2000 program system from Tripos loaded in a Pentium based PC was used. PM3 semiempirical calculations were made using a RMS gradient of 0.1 kcal/(Å mol) and a 0.001 kcal/Å energy delta of energy using the eigenvector-following routine as a convergence algorithm in the restricted Hartee-Fock form.

Synthesis of a 4-[[pentenyl]oxy]-cyanobenzene](I)

A mixture of 5-bromo-1-pentene (25 g, 0.17 mol), 4-cyanophenol (24.8 g, 0.2 mol), acetone (200 mL), and anhydrous potassium carbonate (35.5 g, 0.25 mol) were refluxed for 24 h at 50°C under mechanical stirring. Reaction mixture was poured into water, acetone removed by evaporation, and the aqueous layer extracted with ether (40 mL, 4×). The ether layer was washed with aqueous potassium hydroxide (2*M*, 70 mL, 7×), water (40 mL, 4×), and saturated brine (20 mL, 2×) and then dry using anhydrous sodium sulfate. After ether removal, an yellow oil was obtained which was purified by distillation at reduced pressure; fp 4–9°C, bp 302–309°C (11.4 mg), yield 60%.

FTIR (neat): 2938 (CH_3), 2864 (CH_2), 2223 (CN), 1640 and 916 ($CH{=}CH_2$), 1605 and 1508 (*p*-substituted aromatic), 1258 (C—O—C), 1171 (C—O), 834, 704, and 508 cm^{-1} (*para*-substituted aromatic ring deformation bands).

^{1}H-NMR ($CDCl_3$): δ 7.59–6.88 (AA'BB', 4 H, aromatic), 5.81, 5.10–4.97 (m-, 3 H, -vinyl), 4.00 (t, 2H, —OCH_2), 2.24, 1.89 (m, 4 H, —CH_2CH_2). ^{13}C-NMR ($CDCl_3$): δ 119.23 (CN), 103.29 (NC—C, aromatic), 133.9 (=C—, aromatic), 115.50 (=CH_2, vinyl), 137.28 (CH, vinyl), 115.12 (—C=, aromatic), 162.30 (O—C, *para*-substituted aromatic ring), 67.45 (O—CH_2), 28.03, 29.88 (CH_2—CH_2).

Raman: 3070 (CH, aromatic), 2217.74 (CN), 1567.68 (*p*-aromatic), 1165.20 and 829.42 (aromatic), 1636.58 (vinyl), 642.16 and 474.27 cm^{-1} (C—O—C).

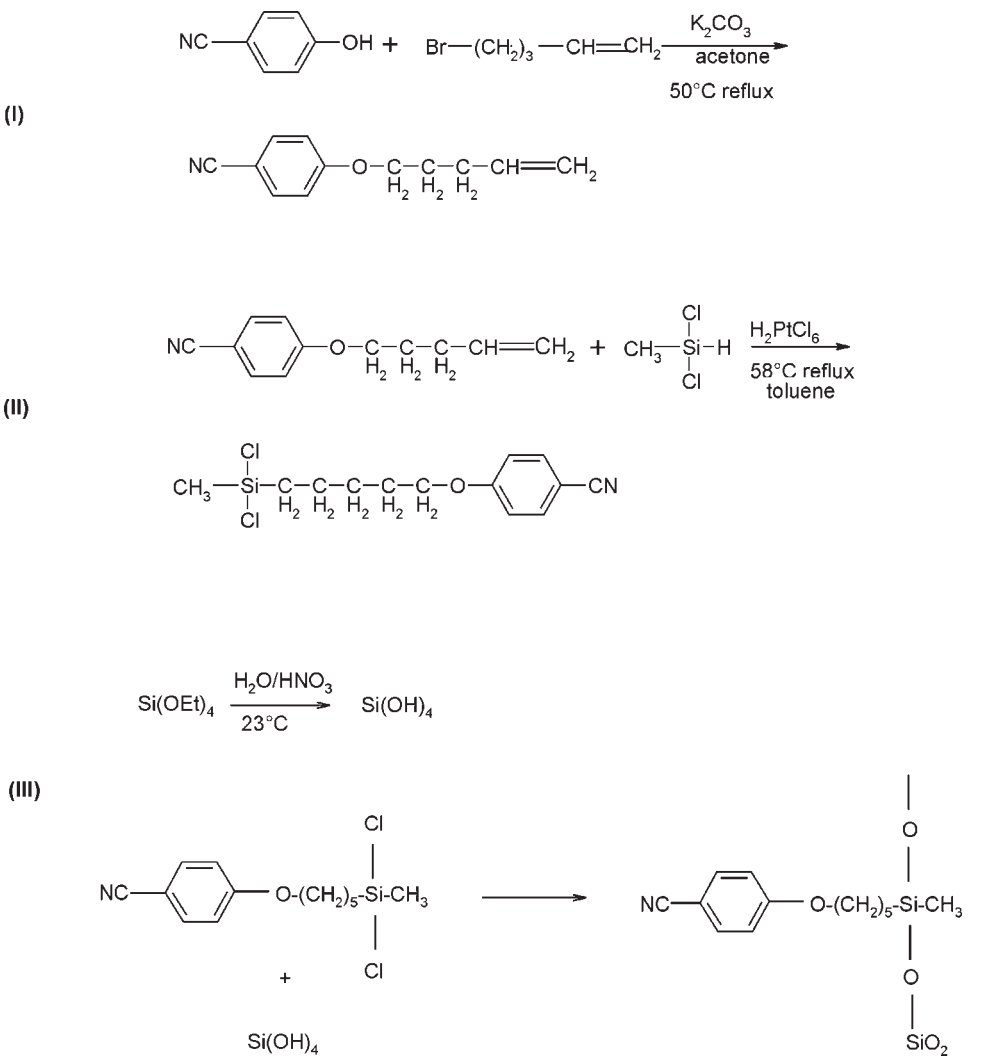

Scheme 1 Chemical route for the synthesis of hybrid materials.

Fluorescence: emission 366 and 658 nm with excitation at 334 nm. Refraction index: 1.534.

Synthesis of 4-[[5-dichloromethylsilyl]pentyl]oxy]-cyanobenzene (DCN)(II)

I (0.005 mol, 0.9362 g.), chloroplatinic acid (THF solution 0.122*M*, three drops), toluene (5 mL), and dimethyldichlorosilane (0.5 mL, 0.005*M*) mixture was heated at 58°C for 16 h. Reaction mixture was cooled and was concentrated up to 20% wt under nitrogen flow and kept in toluene to prevent decomposition by oxygen. A brown liquid was obtained at a yield of 80% (calculated from dry weight). Fb −1.30°C.

II decomposes at 96.6°C. FTIR (neat): 2938 (CH_3), 2864 (CH_2), 2224 (CN), 1606 and 1508 (*p*-substituted aromatic), 1301 (*R*—O—aromatic), 1260 (Si—CH_3), 1172 (C—O), 834 and 508 (*para*-substituted aromatic ring deformation bands), 807 (Si—CH_3), 732 and 696 (Si—CH_2), 480 cm^{-1} (Si—Cl_2).

^{1}H-NMR ($CDCl_3$): δ 7.59–6.88 (AA'BB', 4 H, aromatic), 4.00 (t, 2H, —OCH_2), 189, 1.15 (m, $(CH_2)_4$), 0.79 (3H, —CH_3). ^{13}C-NMR ($CDCl_3$): δ 119.23 (CN), 103.29 (NC—C, aromatic), 133.9 (=C—, aromatic), 115.12 (—C=, aromatic), 162.30 (O—C, *para*-substituted aromatic ring), 67.45 (O—CH_2), 29–21.5 ($(CH_2)_4$), 5.8 (Si—CH_3). ^{29}Si-NMR ($CDCl_3$, INEPT) 32.6 (CH_3—*Si*—).

Raman: 3070 (CH, aromatic), 2902 (CH_3), 2966 (CH_2 sym, asym), 2217 (CN), 1567 (*p*-aromatic), 1165 and 829 (aromatic), 642.16 and 474.27 (C—O—C), 855, 803 (Si—Cl), 739 (Si—CH_2), 538 cm^{-1} (Cl—Si—CH_3).

Fluorescence: emission 413 and 660 nm with excitation at 335 nm.

Synthesis of organic–inorganic glass hybrids

TEOS and THF were slowly mixed at room temperature for 15 min, and then, nitric acid and distilled

water (50 μL/min) were added. Solution of **II** in toluene was poured drop wise under continuous stirring at 23°C, maintaining nitrogen atmosphere during addition. A TEOS/THF/H_2O of 1/3/7*M* ratio was used. The obtained hybrids were carefully dried at room temperature and isolated as monoliths. Hybrid A was obtained from a TEOS/DCN : HNO_3 molar ratio of 1/0.7 : (3% vol). For hybrid B, a TEOS/DCN : ratio of 1/0.7 : (3% vol) was used. Scheme 1 depicts the synthetic route to obtain the hybrids.

FTIR (neat) 3466 cm^{-1} (Si—OH), 2938, 2864 cm^{-1} (CH_3, CH_2), 2228 cm^{-1} (CN), 1606 and 1510 cm^{-1} (*p*-substituted aromatic), 1304 (*R*—O—Ar), 1264 cm^{-1} (C—O—C), 1174 (C—O), 1108y 1078 cm^{-1} (Si—O—Si), 834 (aromatic -H deformation), 548 (Ar—CN), 706 (Si—CH_2).

^{1}H-NMR ($CDCl_3$ before gelation): δ 7.52–6.95 (AA'BB',4 H, *para*-substituted aromatic ring), 4.02 (2 H, —OCH_2—), 1.96, 1.76, 1.30 (3m, $(CH_2)_4$), 0.65 (Si—CHB_2), 0.17 (Si—CHB_3), solvents: THF (3.82, 1.92), Ethanol (3.77), Toluene (7.24, 2.40), acetone (2.21).

^{13}C-NMR ($CDCl_3$ before gelation): δ 119.23 (CN), 103.71 (NC—C, *para*-substituted aromatic ring), 134.07 (=C—, aromatic), 115.33 (—C=, aromatic), 162.54 (C—O, aromatic), 68.51 (O—CH_2), 31.06, 28.97, 23.03 ($(CH_2)_4$), −0.321 (Si—CH_3). ^{29}Si-NMR ($CDCl_3$ before gelation, INEPT): δ −20.12, −20.27. −22.44, −23.11 (cyclic D units), −64.34 (T^2 units).

Raman (solid): 3074.4 (CH, *para*-substituted aromatic ring), 2896.8 (CH_3), 2230.8 (CN), 1609.2 (1,4 aromatic), 1461, 647.2 y 477 (C—O—C), 1313.2, 1246 (Si—CH_3), 1180 (Si—CH_2), 847, 765.6, 736 (Si—O—Si), 477 (C—O—C) cm^{-1}.

Fluorescence emission observed at 395, 550, and 770 nm with wavelength excitation at 330 nm.

Elemental analyses: Hybrid A, calculated (%C = 37.28, %H = 4.06%, %N = 3.34, %O = 29.49, %Si = 25.8), obtained (%C = 30.92, %H = 4.4%, %N = 2.71), Hybrid B, calculated (%C = 46.88, %H = 5.1%, %N = 4.2, %O = 23.34, %Si = 20.43), obtained (%C = 43.7, %H = 5.2%, %N = 4.23).

RESULTS AND DISCUSSION

High resolution ^{29}Si-NMR spectroscopy is a useful technique to determine the structure and microstructure of silicon derivatives. In the study of silicon-containing hybrids, this technique can be used to characterize the silicon species present in the original solution and during the formation of the gel. In solution NMR, silicon-29 nucleus is very difficult to observe because (a) spin-lattice relaxation times are very long (T1 > 20 s for most ^{29}Si nuclei) and (b) low value of magnetogyric ratio ($\gamma = -5.314 \times 107$ rad T^{-1} s^{-1}). One way to overcome these troubles is the use of the sequence insensitive nuclei enhanced by polarization transfer (INEPT).[21,22] The sequence allows simultaneous polarization transfer from all protons to silicon with the same coupling and number of attached protons. Peak enhancements using INEPT are considerable for low γ nucleus such as ^{29}Si-NMR.[23]

Intermediates formed at different times were analyzed by ^{29}Si-NMR using INEPT sequence.[24] The silyl group of the DCN [$(CH_3)Si(R)Cl_2$, R = $(CH_2)_5OC_6H_4CN$] units appears at 32.6 ppm. The siloxane oligomers corresponding to D oligomeric cyclic units (—O—R1—Si—R2—O—),[24] appear between −20 and −40 ppm. Cyclic and linear copolymer species formed during copolymerization were identified as D*n*Q*m*(*i*), where *n* and *m* are the number of DCN [—O—(CH_3)Si(R) —O—] and hydrolyzed TEOS units [Q_1 = —(SiO_4H_3)—, Q_2 = —(SiO_4H_2)—, Q_3—(SiO_4H)— or/and Q_4 = —(SiO_4)—] present in the copolymer (*n* and *m* vary from 1 to 3), and *i* indicates if the species is linear (l) or cyclic (c).

To characterize the chemical species present in hybrids, solid-state ^{29}Si-NMR was used. In hybrid A [see Fig. 1(a)], three broad bands are observed: one at −5.7 ppm due to D_n units, other at −92.5 ppm assigned to the Q_m group of D_nQ_m copolymer, and a peak at −101.4 ppm corresponding to Q^4 units. The same signals are seen in the spectrum of hybrid B at −8.1, −92.5, and −100.1 ppm, respectively. Corresponding signals are also present in the ^{29}Si-NMR CPMAS spectrum of the hybrids [see Fig. 1(b)]. The observed peak patterns closely resemble to those reported for a hybrid obtained from DMS and TEOS.[24] Q_m/Q_4 ratio for hybrid A (1.23) in the CP-MAS spectrum is higher than that for hybrid B (0.76) as a consequence of the low acid concentration (slower rate of hydrolysis) used to obtain hybrid A. The lower value of the ratio Q_m/Q_4 recorded for hybrid B suggests a more crosslinked structure (as a result of the condensation reactions) and a lower content of "free" hydroxyl groups.

Thermal transitions

The thermal study included DSC and Thermogravimetric analysis (TGA) for both DCN and hybrids materials. To know the nature of signals, we also used the first derivative curves. Figure 2(a) shows the DSC thermogram of DCN: a small exothermic peak at 24°C attributed to DCN monomer, a sharp endothermic peak at 53°C corresponding to formation of cyclic oligomers, and a broad endothermic peak at about 129°C (ΔH = −4.13 J/g) attributed to the formation of DCN linear oligomers.

The first derivative curve of the DCN monomer [Fig. 2(b)] shows the peaks mentioned above and some small peaks between 60 and 110°C attributed to the formation of intermediates.

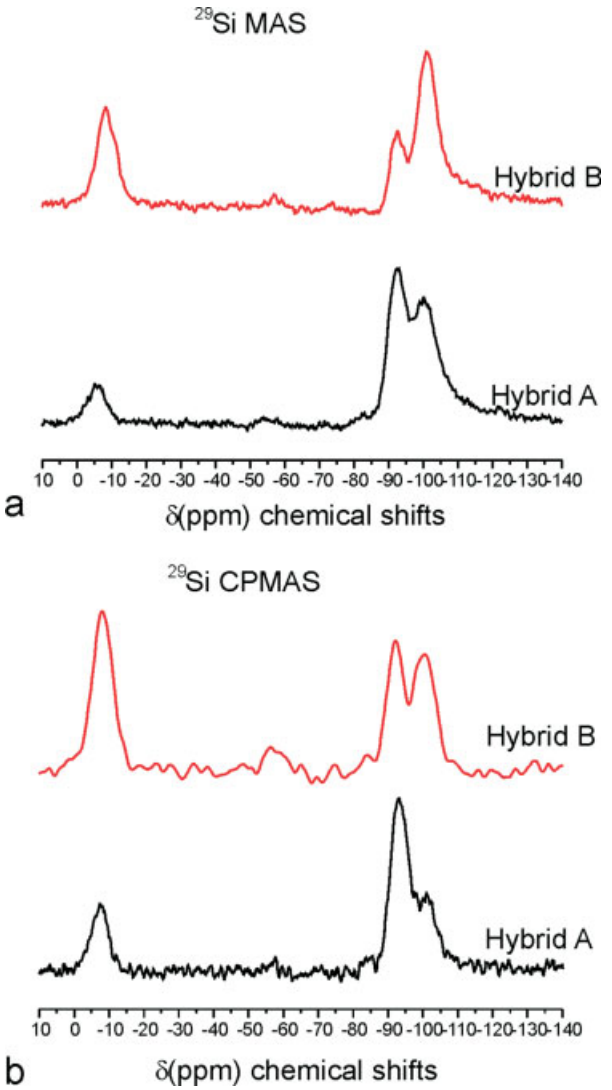

Figure 1 Silicon-29 solid-state NMR spectra of hybrids: (a) MAS (top) and (b) CPMAS (bottom). [Color figure can be viewed in the online issue, which is available at www.interscience.wiley.com.]

Figure 2 also shows the DSC thermogram of DCN oligomers (formed in the presence of water); a small exothermic signal at about 23.5°C appearing in the first heating indicates that some DCN monomer was still present. This peak did not appear in the second heating, suggesting total conversion of DCN monomer after first heating. The endothermic peak at 54°C, present in both heating cycles, corresponds to the oligomeric cyclic units. Observe that in the second heatings no signal appears at 128°C, indicating that only cyclic oligomers are mainly formed during DCN oligomerization induced by water.[24,25]

It has been reported that T_g temperatures of polymers containing silica depend on the silica content.[26–28] This dependence was observed only in those cases where the polymer is not chemically bound to the silica lattice. In hybrids, the reaction between DCN units and silica results in formation of Si—O—Si units. Crosslinking reactions also lead to the formation of more Si—O—Si bonds.

Formation of Si—O—Si bonds was studied by FTIR before and after DSC analyses of DCN monomer, and the spectra were compared with that of the oligomers. Figure 3 shows signal assignment of DCN monomer peaks as well as the Si—O—Si peaks resulting from chemical bonding of DCN to silica. The Si—O—Si peaks in cyclic oligomers can be distinguished form those in linear oligomers. Broad signals, assigned to cyclic {1077 cm^{-1}, $D_2Q_1(c)$, $D_3Q_1(c)$, $D_2Q_2(c)$[24]} and linear oligomers {3439 and 1077 cm^{-1m}, $D_1Q_1(l)$, $D_2Q_1(l)$, $D_2Q_2(l)$, $D_4Q_4(l)$,[24]}, can be observed. The FTIR spectra of the DCN oligomers only shows evidence of cyclic siloxane units (peak at 1077 cm^{-1}), no Si—OH functionality was observed, (3439cm^{-1}). As it has been reported, solution ^{29}Si-NMR for oligomers only shows peaks due to cyclic units.[24,25]

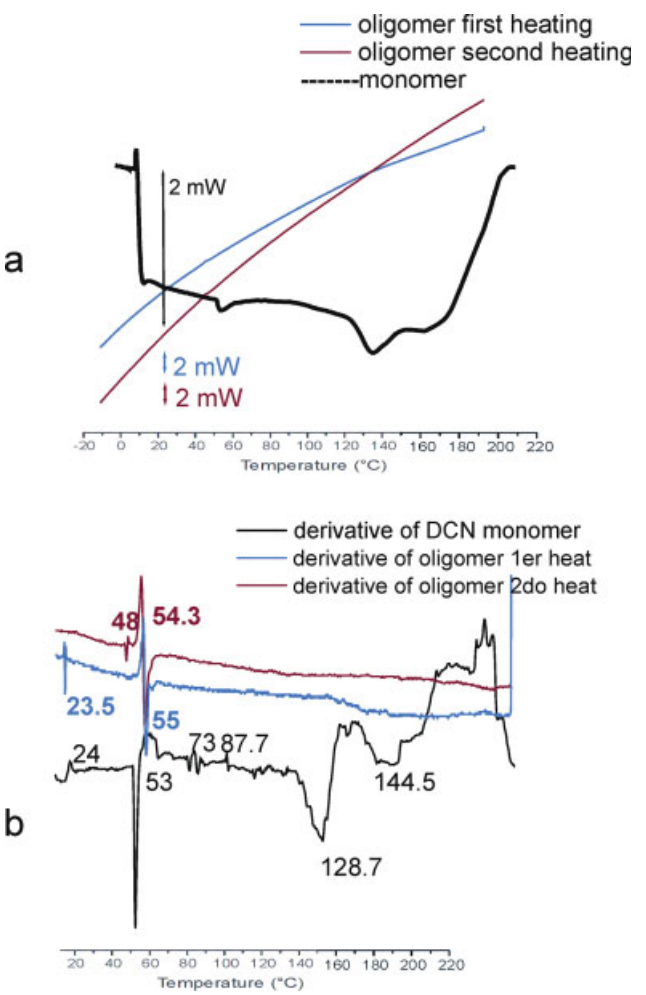

Figure 2 DSC thermograms of DCN oligomer and DCN monomer. [Color figure can be viewed in the online issue, which is available at www.interscience.wiley.com.]

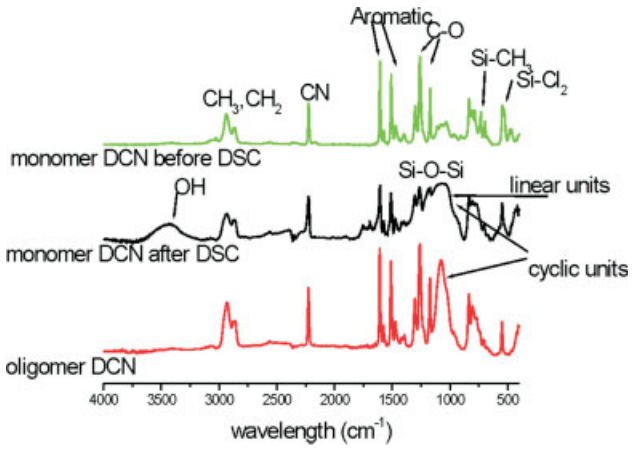

Figure 3 FTIR spectra of oligomers and monomer DCN before and after obtaining the DSC thermogram. [Color figure can be viewed in the online issue, which is available at www.interscience.wiley.com.]

Peak assignments were confirmed by studying the chemical reactions as well as reported FTIR and NMR spectra of DCN.

The elemental analysis shows that hybrid A contains around 15% more silica than hybrid B. Although the difference between the observed T_g temperatures for hybrids is small, a big difference in signal intensity is observed in the DSC thermograms. According to solid-state silicon-29 NMR analysis, there is a higher amount of condensed material in hybrid B than in hybrid A (Fig. 1). These results agree with the DSC peak patterns of both hybrids as shown in Figure 4(a). A wide endothermic peak for hybrid B, centered at 85°C (ΔH = 66.6 J/g), is observed (range 10.6–175°C).

Within this temperature range, dehydration reactions lead to crosslinking according to Scheme 2. In comparison, the thermogram for hybrid A also

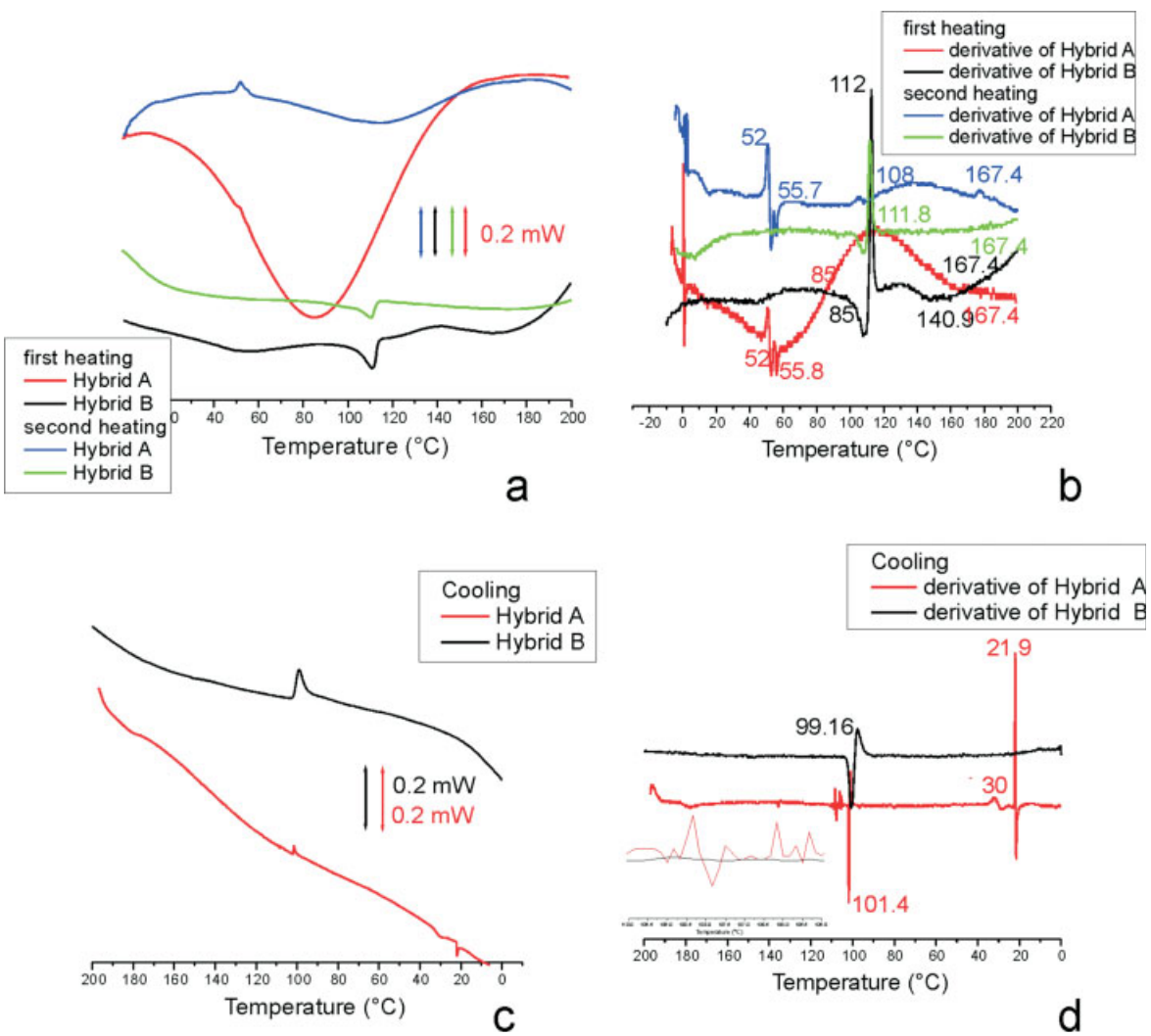

Figure 4 DSC thermograms for hybrid A and hybrid B. [Color figure can be viewed in the online issue, which is available at www.interscience.wiley.com.]

Scheme 2 Condensation reactions that lead to crosslinking in the hybrid. Because of the dependence on heat rates, existence of a microrreversible equilibrium can be proposed.

shows a smooth endothermic signal between 4.6 and 217°C, but with a much lower change in enthalpy (ΔH = 7.3 J/g). These peaks, observed in both hybrids, are attributed to the endothermic chemical reaction between silanol groups to form Si—O—Si bonds (crosslinking).

Hybrid A shows small exothermic peaks at 52.8°C (ΔH = 0.47 J/g), attributed to reordering of cyclic oligomers (probably crystallization).The thermogram of hybrid B does not show peaks around 50°C suggesting that the concentration of cyclic units is very small.

The observed features discussed above are clearly revealed in the first derivative curves, Figure 4(b), even in a second heating analysis. The DSC derivative curves of hybrids A and B, Figure 4b, show a wide exothermic signal for hybrid A and sharp exothermic signal, all at around 110°C. The nature of these signals is discussed next. Figure 4(c) show the cooling DSC thermograms of hybrids A and B. In both, an exothermic peak appears around 100°C with a ΔH of 0.03 J/g for hybrid A and ΔH of 0.5 J/g) for hybrid B. These peaks revealed clearly in the derivative plot, Figure 4(d), correspond to crystallization of linear chains. These crystallization peaks are related to the exothermic peaks appearing at 110°C in Figure 4(b). i. e.; relaxation of linear chains, probably melting in hybrid B.

During second heating, both hybrids show endothermic peaks at around 111°C as shown in Figure 4(a). These peaks are attributed to dehydration reactions that led to crosslinking and linear copolymer formation. These condensation reactions include those groups that remained unreacted during the first heating.

The acid concentration influences the nature of crosslinking reactions and linear copolymer formation. The TEOS/DCN : HNO3*M* ratio for hybrid A was 1/0.3 : (0.3% vol) and for hybrid B was 1/0.7 : (3% vol). The enthalpy, ΔH, involved in the crosslinking reaction of hybrid A at 111°C was higher (3.9 J/g) than that for hybrid B (0.5 J/g). The amount of acid used influences hydrolysis kinetics.

TGA was undertaken to determine useful range temperatures of hybrids. As shown in Figure 5(b) hybrid B loses weight above 140°C, while the loss of weight in hybrid A starts at about 25°C. Therefore, the thermal stability of hybrid B is greater than hybrid A at temperatures below 140°C. Above this temperature, the global rate of decomposition is lower for hybrid A because of its lower content of DCN. Apparently, the rate of decomposition decreases as silica density is increased. The TGA of a sol–gel glass, as obtained directly from TEOS,[24] was included to compare its thermal behavior with the hybrids. As expected, the sol–gel glass loss water below 100°C after this temperature the resulting glass is completely stable.

Differential thermal analysis (DTA) was used to detect desorption in hybrids. As shown in Figure 5(b), no endothermal peaks are observed suggesting absence of desorption in hybrids. This might be an indication that DCN units are strongly attached to silica through the siloxane bonds.

To learn more about the thermal and chemical behavior of hybrids, new DSC experiments were run after aging the hybrids for one year at room temperature in closed vials. The thermograms (heating and reheating) of aged hybrid A, Figure 6(a) and first

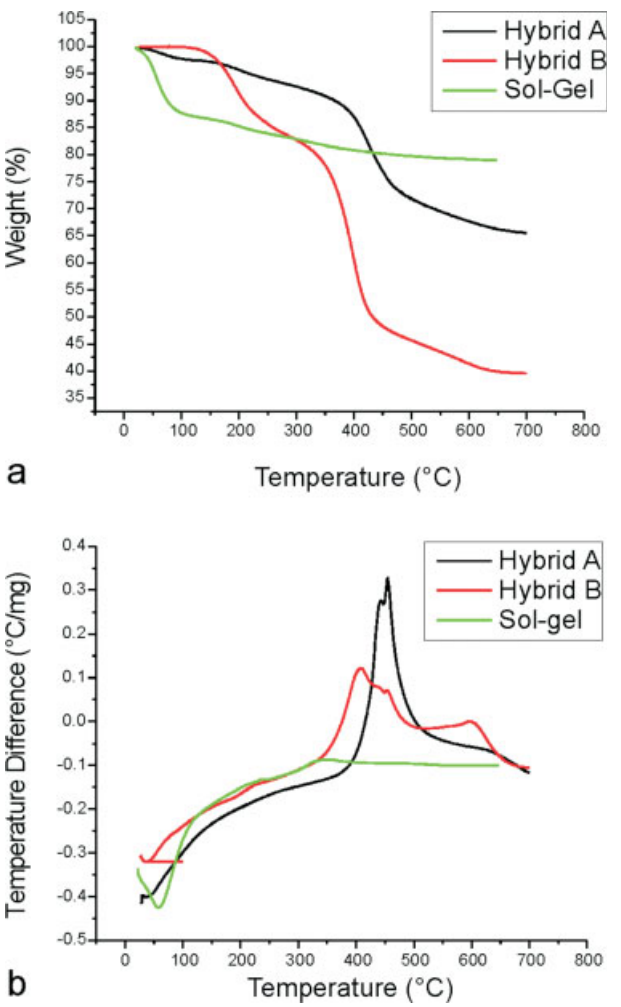

Figure 5 (a) TGA and (b) DTA thermograms for hybrids A and B and for sol–gel glass. [Color figure can be viewed in the online issue, which is available at www.interscience.wiley.com.]

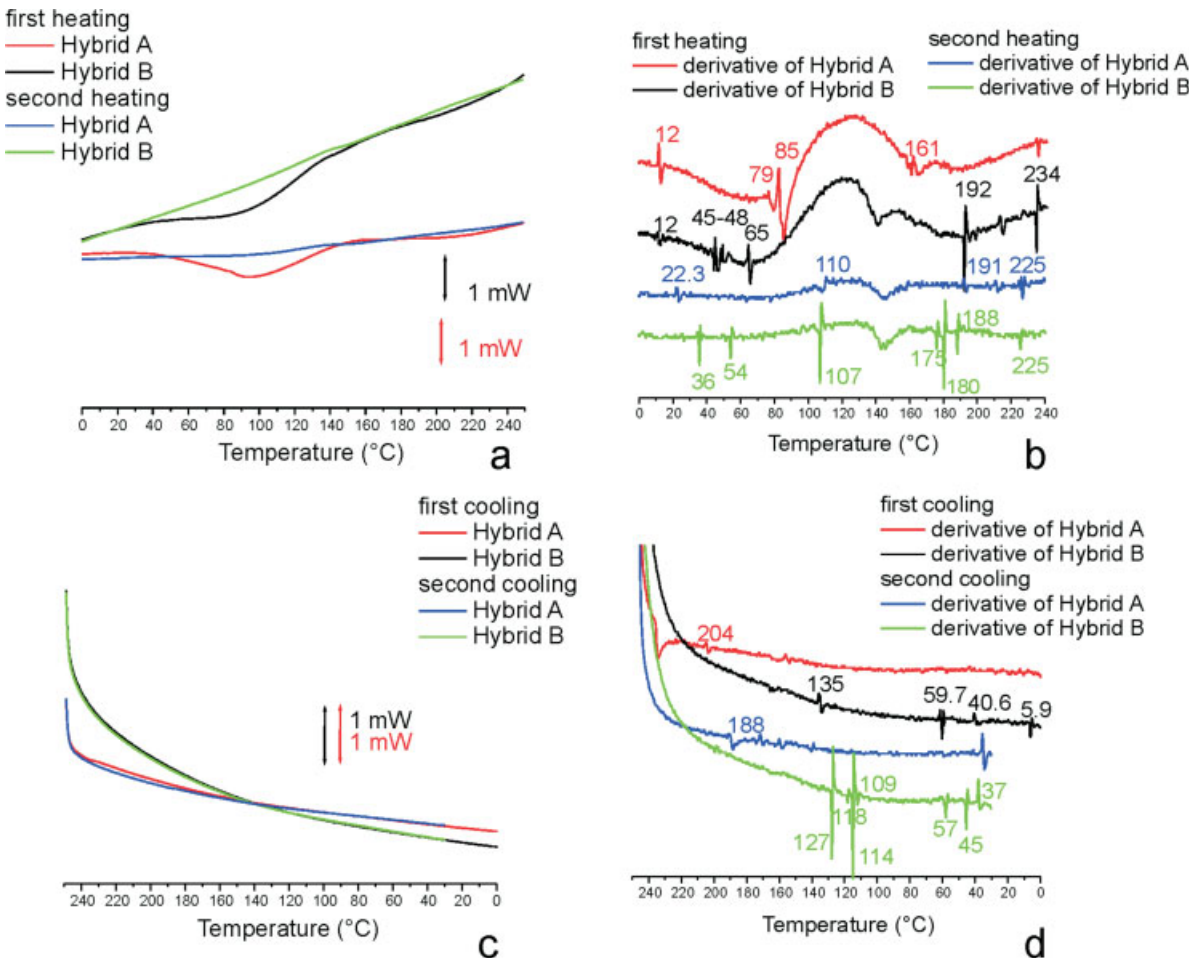

Figure 6 DSC thermograms for aged hybrids A and B. [Color figure can be viewed in the online issue, which is available at www.interscience.wiley.com.]

derivatives, Figure 6(b), shows a main endothermic transition at 85°C (ΔH = 4.2 J/g) assigned to the crosslinked polymer and secondary transitions at 12, 79, and 161°C, assigned to relaxations of cyclic and linear oligomers. Hybrid B, shown in the same figures, presents a similar behavior. A main endothermic transitions at 94°C (ΔH = 0.57 J/g), and secondary transitions at 12, 45, 48, and 65°C. The transitions above 140°C correspond to thermal degradation.

The enthalpy (ΔH) involved in the main transitions of aged hybrids is lower than the measured in recently made hybrids. These results indicate that aging increases the thermal and chemical stability of hybrids.

Upon cooling, no main transitions are observed below 140°C, Figure 6(c). The derivative curves, Figure 6(d), show secondary transitions assigned to reordering, probably crystallization of linear copolymers and cyclic copolymers. The crystallization peak of recently made hybrids, observed at 110°C in Figure 4(c), is very small in aged hybrids.

During second heating of hybrids A and B, the main transitions at 110°C and 107°C, respectively, are quite small as well as the secondary transitions. In general, the higher amount of DCN, as in hybrid B, results in higher intensities in the DSC signals.

It can be observed that there are higher slopes for hybrid B than for hybrid A, Figure 6(a,c) of the curve. These differences in aged hybrids are attributed here to: (a) differences in hybrid heat capacities and (b) crosslinking.

According to our interpretation, the transitions observed below 70°C are due to cyclic copolymers and oligomers, whereas those between 85 and 113°C correspond to linear copolymers. Transitions above 140°C are due to loss of weight. It is expected that occurrence of crosslink reactions be lower for hybrid B, as DCN forms D*n*Q*m* units in hybrids that contain less "free" silanol groups. Segments with a more content of hydrolyzed TEOS units more likely produce Si—O—Si bonds by condensation reactions.

Figure 7 shows a thermogram of aged hybrid A and its first derivative, obtained at a heating rate of 2°C/min. The main endothermic peak is observed now at 69.3°C (ΔH = 30.1 J/g). At a heating rate of 10°C/min, the peak is at 85°C as observed in Figure

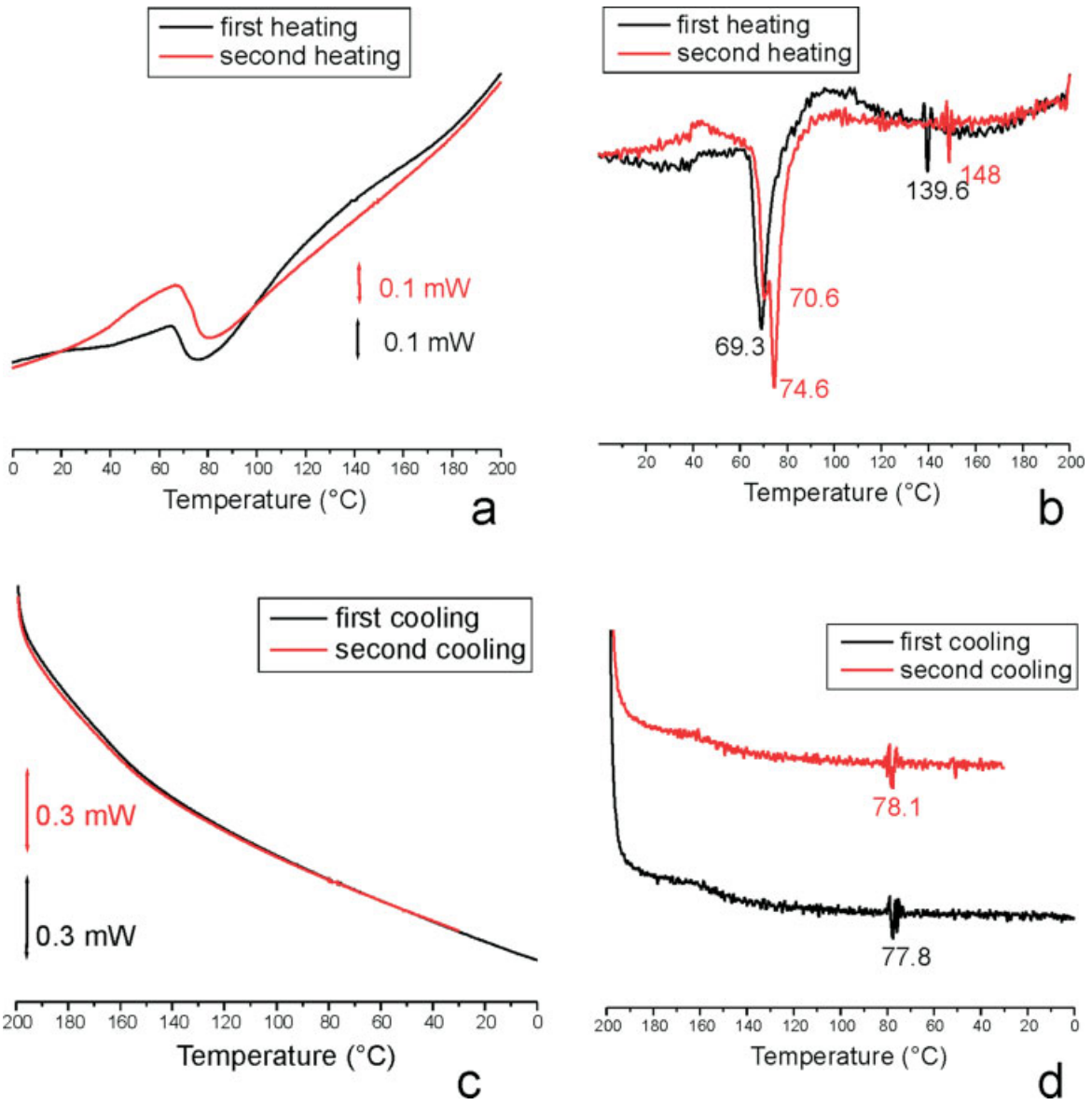

Figure 7 DSC thermograms for aged hybrid A at a heat rate of 2°C/min (a and c) and the corresponding derivative curves (b and d). [Color figure can be viewed in the online issue, which is available at www.interscience.wiley.com.]

4(a). A similar behavior is observed on cooling. At lower heating rates, equilibria between the different species involved in the crosslinking reactions take place, lowering the heat evolved by condensation reactions.

As expected, at lower heating rates, the transitions occur at lower temperatures and equilibrium between the different species involved take place.

Morphology

Wide angle X-ray diffraction spectra were obtained to determine the presence of ordered structures in hybrids. It can be observed in Figure 8 that both hybrids show coherent peaks at 3.8° and 21°; Bragg angle (2θ). These peaks suggest the presence of ordered–disordered phases.

A diffractogram for silica (SiO_2), as obtained directly from TEOS by sol–gel reactions,[24] was included in Figure 8 for comparison. A broad diffuse peak centered at 24°, characteristic of an amorphous phase, is observed. The peak at 3.8° suggests the presence of ordered phases similar to those reported for fluid-like liquid crystal mesophases. In particular, a similar peak is reported for ferroelectric polysiloxanes having a smectic mesophase (S_c* arrangement).[22,25,29] This peak corresponds to molecular arrays with a regular spacing around 23 Å. We previously reported ordered arrays based on atomic force microscopy (AFM) and transmission electronic

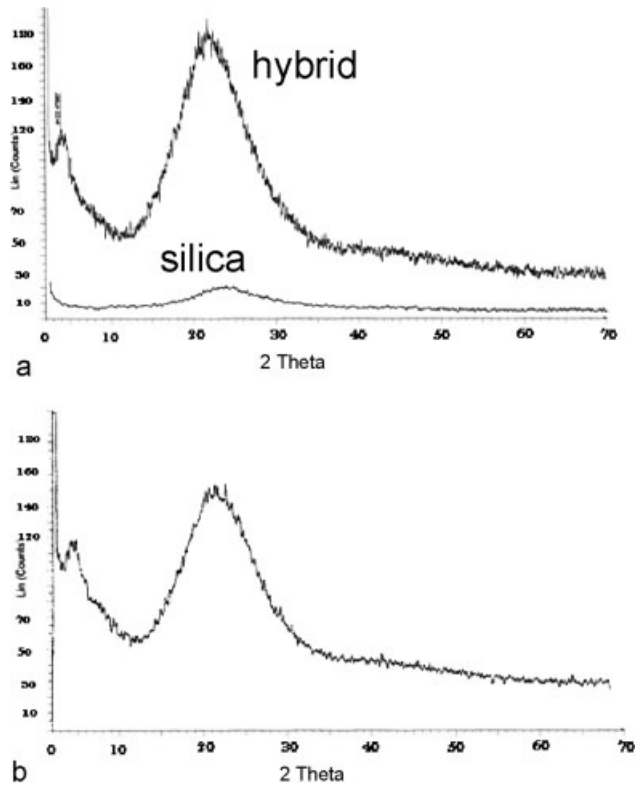

Figure 8 Wide-angle X-ray diffraction pattern of: (a) Hybrid A and (b) Hybrid B. The diffractogram of silica is also shown for comparison.

microscopy (TEM) micrographs.[24] The photographs evidence the existence of ordered bands separated by 50 to 100 nm. The observed spacing corresponds to the dimensions of mesospheric arrangements present in the hybrids.

Optical properties

One of the most common ways to detect nonlinear optical properties in materials is to measure the variation of the refractive index, n, as a function of light intensity I (this is the so-called nonlinear refractive index). Figure 9 depicts the set-up used for studying the optical properties of hybrids as well as the observed pattern obtained after a continuous-wave laser beam of about 20 mW (argon laser at 514 nm) focused onto the sample. The emerging beam expands with a very large angular divergence into a pattern of concentric luminous rings, which could be observed on a screen. The observed pattern arises as a consequence of light modification due to self-generated refractive index occurring in the focal spot. This phenomenon in NLO materials has been named "self-diffraction." Both hybrids (A and B) showed this diffraction pattern, indicating that they possess nonlinear optical properties. Similar patterns are recorded for liquid crystal materials and dye doped films.[30,31]

Molecular modeling

The minimum-energy structure of an idealized section of the copolymer made from DCN and TEOS was obtained as described in the experimental section. The minimum-energy structure, shown in Figure 10 simulates a siloxane copolymer section containing a pentyl-oxy-cyanobenzene moiety (mesogenic unit), along with silicate bonds. It is well known that pentyl-oxy-cyanobenzene is a chromophore that could impart nonlinear optic properties to hybrids.[32] In this minimum-energy structure the chromophore is attached to the main polysiloxane chain as a pendant group. It should be mentioned that siloxane oligomers of DCN are viscous liquids at room temperature. These oligomers are amorphous structures with viscoelastic properties. They do not align to form mesophases because they are not rigid enough to form molecular rods. However, the pendant pentyl-oxy-cyanobenzene groups in the hybrids behave differently. Here, the chromophores, attached to flexible polysiloxane chains, form the mesogenic phase. Internal rotations along the main siloxane copolymer make possible to accommodate the chromophores in ordered structures, having a liquid crystal like behavior.[33]

CONCLUSIONS

Thermal and optical characterization of two organic–inorganic hybrids, obtained from 4-[[5-dichloromethylsilyl]pentyl]oxy]-cyanobenzene (DCN) and tetraethoxysilane (TEOS), is reported in this work. The hybrids are mainly composed of a siloxane

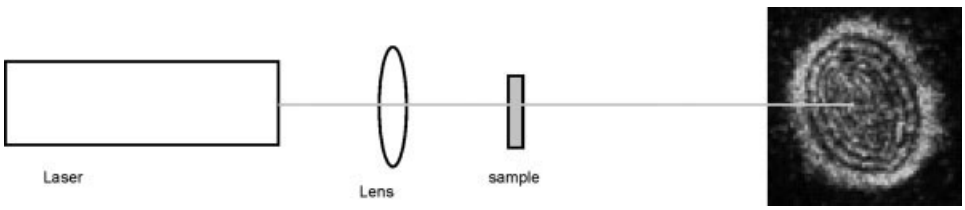

Figure 9 Experimental set-up for the optical analysis of hybrids. A typical self- diffraction pattern of concentric luminous rings obtained from hybrid *A* is shown at the right hand side.

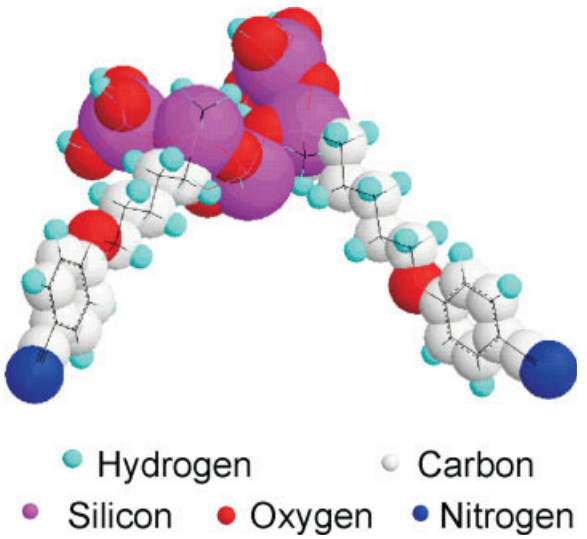

Figure 10 Minimum-energy structure for an idealized section of the copolymer. [Color figure can be viewed in the online issue, which is available at www.interscience.wiley.com.]

copolymer with silicate units. The copolymer forms a network resulting from crosslinking, and it has pendant groups of pentyl-oxy-cyanobenzene that behave as chromophores. Presence of reaction intermediates during chemical reactions was detected. Therefore, a precise control of reaction conditions was exerted to obtain good-quality glasses (hybrids).

These materials show several thermal transitions but do not decompose below 200°C. Several physical changes and chemical reactions are observed in hybrids during thermal treatment. These changes were assigned considering monomer and oligomers DSC thermograms. First-derivative curves aid in the identification of transitions. In summary, observed differences in the peaks attributed to crosslinking reactions can be explained in terms of copolymer composition and the amount of used acid (which influences hydrolysis kinetics).

Hybrids present ordered–disordered phases as detected by WAXS. Ordered phase has a mesogenic structure containing the siloxane copolymer. The disordered phase is mainly silica glass domains. Molecular modeling of an idealized copolymer chain suggests that pendant pentyl-oxy-cyanobenzene groups arrange as rigid rods forming liquid crystal-like structures.

Hybrids A and B present self-diffraction patterns forming coherent rings. Observed patterns are typical of materials with NLO properties. This indicates that hybrids A and B may be amenable for electro-optic applications.

The authors are indebted to the reviewer for his valuable suggestions to improve the quality of the article.

References

1. http://investintaiwan.nat.gov.tw/en/news/200506/2005062901.html. Accessedon September 2005.
2. Loy, D. A.; Shea, K. J. Chem Rev 1995, 95, 1431.
3. Sellinger, A.; Laine, R. M. Macromolecules 1996, 29, 2327.
4. Altman, J. C.; Stone R. E. SPIE Sol-Gel Optics II 1992, 1758, 507.
5. Harreld, J. H.; Dunn, B.; Zink, J. I. SPIE 1997, 3136, 25.
6. Laczka, M.; Cholewa-Kowalska, K.; Kogut, M. J Non-Cryst Solids 2001, 287, 10.
7. Han, Y.; Lin, J.; Zhang, H. Mater Lett 2002, 54, 389.
8. Levy, D.; Quintana, X.; Rodrigo, C.; Oton, J. M. SPIE Sol-gel Optics III 1994, 2288, 529.
9. Andrews, M. P. SPIE Integr Optics Dev; Potential Commercialization 1997, 2997, 48.
10. Burzynski, R.; Castevens, M. K.; Zhang, Y. Zieba, J.; Prasad, P. N. SPIE Org Biol optoelectron 1993, 1853, 158.
11. Boilot, J-P.; Biteau, J.; Chaput, F.; Giacoin, T.; Brun, A.; Darracq, B.; Georges, P.; Levy, Y. Pure Appl Opt 1998, 7, 169.
12. Dalton, L. R.; Harper, A. W.; Zhu, J.; Steier, W. H.; Salovey, R.; Wu, J.; Efron, U. SPIE 1995, 2528, 106.
13. Gurney, J. A.; Vargas-Baca, I.; Brown, A. P.; Andrews, M. P.; Najafi, A. I. SPIE Org-Inorg Hybrid Mater Photonics 1998, 3469, 145.
14. Levy, D. SPIE Sol-Gel Optics IV 1997, 3136, 77.
15. Levy, D. Pure Appl Opt 1996, 5, 621.
16. Levy, D. SPIE Sol-Gel Optics V 2000, 3943, 26.
17. Pope, E. J. A. SPIE-Sol-Gel Optics III 1994, 2288, 537.
18. Ramirez -Niño, J.; Lopez-Mancilla, A.; Perez-Abad, C.; Rodríguez, J. H.; Rejon, L.; Nava, R.; Castaño, V. M. Int J Polym Mater 1997, 37, 217.
19. Zhang, Y.; Cui, Y. P.; Wung, C. J.; Prasad, P. N. SPIE Nonlinear Opt Properties Org Mater IV 1991, 1560, 264.
20. Kumar, S. Liquid Crystals, Experimental study of physical properties and phase transitions; Cambridge University Press: Cambridge, UK, 2001, p 393.
21. Morris, G. A.; Freeman, R. JACS 1979, 101, 760.
22. Doddrell, D. M.; Pegg, D. T.; Brooks, W.; Bendall, R. 1981, 103, 727.
23. Sanders, J. K. M.; Hunter, B.K. Modern NMR Spectroscopy; Oxford University Press: Oxford, 1993, p 88.
24. Trejo-Durán, M.; Martinez-Richa, A.; Vera-Graziano, R.; Mendoza-Diaz, G.; Castaño-Meneses, V. M. J Appl Polym Sci 2006, 99, 473.
25. Marsmann, H. In NMR Basic Principles and Progress; Diehl, P., Fluck, E., Kosfeld, R., Eds.; Springer: Berlin, 1981, pp 97–197.
26. Imai, Y.; Yoshida, N.; Naka, K.; Chujo, Y. Polym J 1999, 31, 258.
27. Kweon, J-O.; Noh, S. J Appl Polym Sci 2001, 81, 2471.
28. Tong, X.; Tang, T.; Zhang, Q.; Feng, Z.; Huang, B. J Appl Polym Sci 2002, 83, 446.
29. Hu, Y. J Mater Sci 2000, 25, 3155.
30. Potes, H.; Zentel, R. Liq Cryst 1994, 16, 749.
31. Gurke, I.; Wultz, C.; Giesseler, D.; Janssens, B.; Heidelbach, F.; Riekel, C.; Kricheldof, H. R. J Appl Crystallogr 2000, 33, 718.
32. Nalwa, H. S.; Miyata, S. Non linear Optics of Molecules and Polymers; CRC Press: USA, 1997, pp 89–122.
33. DeGennes, P. G.; Prosa, J. The Physics of Liquid Crystals, 2nd ed.; Oxford University Press: UK, 1993.